

This is the accepted manuscript made available via CHORUS. The article has been published as:

Efimov Physics in Quenched Unitary Bose Gases

José P. D’Incao, Jia Wang, and V. E. Colussi

Phys. Rev. Lett. **121**, 023401 — Published 9 July 2018

DOI: [10.1103/PhysRevLett.121.023401](https://doi.org/10.1103/PhysRevLett.121.023401)

Efimov Physics in Quenched Unitary Bose Gases

José P. D’Incao,^{1,2} Jia Wang,³ and V. E. Colussi^{1,2,4}

¹*JILA, University of Colorado and NIST, Boulder, Colorado 80309-0440, USA*

²*Department of Physics, University of Colorado, Boulder, Colorado 80309-0440, USA*

³*Centre for Quantum and Optical Science, Swinburne University of Technology, Melbourne 3122, Australia*

⁴*Eindhoven University of Technology, PO Box 513, 5600 MB Eindhoven, The Netherlands*

We study the impact of three-body physics in quenched unitary Bose gases, focusing on the role of the Efimov effect. Using a local density model, we solve the three-body problem and determine three-body decay rates at unitarity, finding density-dependent, log-periodic Efimov oscillations, violating the expected continuous scale-invariance in the system. We find that the breakdown of continuous scale-invariance, due to Efimov physics, manifests also in the earliest stages of evolution after the interaction quench to unitarity, where we find the growth of a substantial population of Efimov states for densities in which the interparticle distance is comparable to the size of an Efimov state. This agrees with the early-time dynamical growth of three-body correlations at unitarity [Colussi *et al.*, Phys. Rev. Lett. 120, 100401 (2018)]. By varying the sweep rate away from unitarity, we also find a departure from the usual Landau-Zener analysis for state transfer when the system is allowed to evolve at unitarity and develop correlations.

PACS numbers: 31.15.ac, 31.15.xj, 67.85.-d

Over the past few years, the study of strongly interacting Bose gases has greatly intensified due to the experimental advances with ultracold atoms [1–10], unraveling universal properties and other intriguing phenomena [11–32]. Although ultracold quantum gases have extremely low densities, n , the unique ability to control the strength of the interatomic interactions —characterized by the s -wave scattering length, a — via Feshbach resonances [33] allows one to probe the *unitary regime* ($n|a|^3 \gg 1$), where the probability for collisions can reach unity value and the system becomes non-perturbative. In contrast to their fermionic counterparts [34–36], unitary Bose gases are susceptible to fast atomic losses [37] that can prevent the system from reaching equilibrium. In Ref. [3], a quench of the interactions from weak to strong allowed for the study of the dynamical evolution and equilibration of the unitary Bose gas, thanks to the surprisingly slow three-body decay rates [17]. By making the unitary regime accessible, this new quenched scenario opened up intriguing ways to study quantum few- and many-body non-equilibrium dynamics in a controlled manner [38–43].

Our understanding of how correlations evolve and subsequently equilibrate in quenched unitary Bose gases is evolving as recent experiments probe physics in this regime [1–6, 8–10]. Most of the current theoretical approaches, however, are based on the two-body physics alone, leaving aside the three-body Efimov physics [44–50]. In particular, at unitarity ($|a| = \infty$), although no weakly bound two-body state exists, an infinity of Efimov states form. Critical aspects such as the three-body loss rates and dynamical formation of Efimov state populations remain unexplored within the non-equilibrium scenario of quenched unitary Bose gases.

In this Letter, we explore various aspects related to the three-body physics in quenched unitary Bose gases.

We solve the three-body problem using a simple local model, incorporating density effects through a local harmonic trap and describing qualitatively Efimov physics embedded in a larger many-body system. Within this model, we determine loss rates at unitarity that display density-dependent, log-periodic oscillations due to Efimov physics. We also analyze the dynamical formation of Efimov states when the quenched system is held at unitarity and then swept away to weak interactions. This scheme was recently implemented for an ultracold gas of ^{85}Rb atoms [8], where a population of Efimov states in a gas phase was observed for the first time. Our present study analyzes such dynamical effects and demonstrates that for densities where the interparticle distance is comparable to the size of an Efimov state, their population is enhanced. This is consistent with a recent theoretical study on the early-time dynamical growth of three-body correlations [30], providing additional evidence for the early-time violation of the universality hypothesis for the quenched unitary Bose gases [11]. By studying the dependence of the populations on the sweep time, we find a departure from the usual Landau-Zener model of the state formation as the system evolves at unitarity and develops correlations.

Within the adiabatic hyperspherical representation [51–54], the total three-body wave function for a given state β is decomposed as

$$\psi_\beta(R, \Omega) = \sum_\nu F_{\beta\nu}(R) \Phi_\nu(R; \Omega), \quad (1)$$

where Ω collectively represents the set of all hyperangles, describing the internal motion and overall rotations of the system, and the hyperradius, R , gives the overall system size. The channel functions Φ_ν are eigenstates of the hyperangular part of the Hamiltonian (including all interatomic interactions) whose eigenvalues are the hy-

spherical potentials, obtained for fixed values of R . Bound and scattering properties of the system are determined by solving the three-body hyperradial Schrödinger equation,

$$\left[-\frac{\hbar^2}{2\mu} \frac{d^2}{dR^2} + W_\nu(R) \right] F_\nu(R) + \sum_{\nu \neq \nu'} W_{\nu\nu'}(R) F_{\nu'}(R) = E F_\nu(R), \quad (2)$$

where $\mu = m/\sqrt{3}$ is the three-body reduced mass and ν an index that includes all quantum numbers necessary to characterize each channel. The hyperradial motion is then described by Eq. (2) and is governed by the effective three-body potentials W_ν and nonadiabatic couplings $W_{\nu\nu'}$. In our model, we assume atoms interact via a Lennard-Jones potential, $v(r) = -C_6/r^6(1 - \lambda^6/r^6)$, where C_6 is the dispersion coefficient [33], and λ is a parameter adjusted to give the desired value of a , tuned such that only a single s -wave dimer can exist [55]. The correct three-body parameter [54, 56, 57], found in terms of the van der Waals length $r_{\text{vdW}} = (mC_6/\hbar^2)^{1/4}/2$ [33], is naturally built into this potential model, providing a more realistic description of the problem.

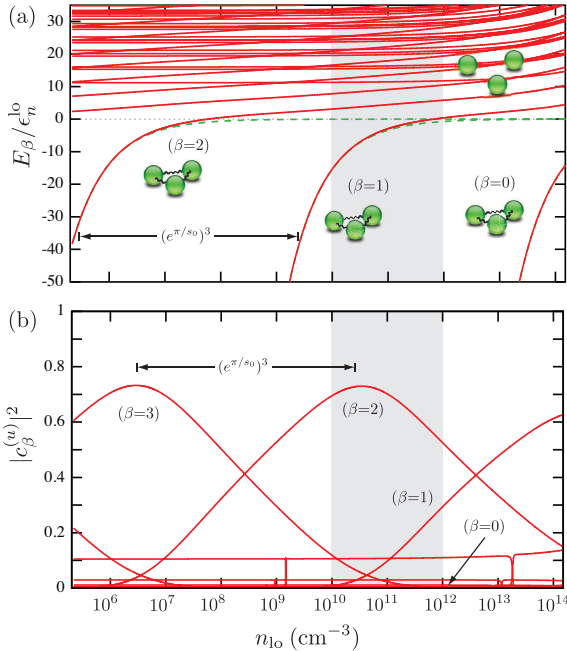


FIG. 1. (a) Energies, E_β [in units of $\epsilon_n^{\text{lo}} = \hbar^2(6\pi^2 n_{\text{lo}})^{2/3}/2m$], of three-identical bosons at $|a| = \infty$ as a function of the local density, n_{lo} . The dashed green lines represent the free space Efimov state energies. (b) The corresponding population of three-body states, $|c_\beta|^2$, for quenching to unitarity. The shaded region marks the range of densities where we have studied the dynamical formation of Efimov states.

In order to qualitatively incorporate density effects in our calculations, we introduce a *local* harmonic confinement whose properties are determined by the av-

erage atomic density, $\langle n \rangle$ [17, 58–60]. This allows us to connect local few-body properties to density-derived scales of the gas, including the system's energy, $\epsilon_n = \hbar^2(6\pi^2 \langle n \rangle)^{2/3}/2m$, length scales, $k_n^{-1} = \hbar/(2m\epsilon_n)^{1/2}$, and time scales, $t_n = \hbar/\epsilon_n$. In the hyperspherical representation, local harmonic confinement is achieved by adding a hyperradial harmonic potential [61, 62],

$$V_{\text{ho}}(R) = \frac{\mu \omega_{\text{ho}}^2}{2} R^2, \quad (3)$$

to the effective potentials W_ν in Eq. (2). Here, $\omega_{\text{ho}} = \hbar/ma_{\text{ho}}^2$ is the trapping frequency and a_{ho} is the oscillator length. A priori, there is no unique way to relate the harmonic confinement in our model to the atomic density. Nevertheless, as shown in Refs. [17, 25, 30, 58–60], calibrating the local trapping potential [Eq. (3)] to match the few-body density with the interparticle spacing ($\sim \langle n \rangle^{-1/3}$) qualitatively describes the larger many-body system for time scales shorter than $t_{\text{ho}} = 1/\omega_{\text{ho}}$. Here, we relate the local atomic density, n_{lo} , and local trapping potential by

$$n_{\text{lo}} = \left[\frac{4\pi}{3} \langle \psi_i | R^3 | \psi_i \rangle \right]^{-1} \propto \frac{1}{a_{\text{ho}}^3}, \quad (4)$$

where ψ_i is the three-body wave function of the lowest trap state in the regime of weak interactions. The results of this Letter were obtained using ψ_i relevant for the ^{85}Rb experiment [8], in which the pre-quench, initial state corresponds to $a \approx 150a_0$.

In free space, and in the absence of a background gas, the energies of Efimov states at unitarity, E_{3b} , accumulate near the free-atom threshold ($E = 0$), and their corresponding sizes, R_{3b} , increase according to the characteristic log-periodic geometric scaling [46]:

$$E_{3b}^{(j)} = -\frac{\hbar^2 \kappa_*^2}{(e^{\pi/s_0})^{2j} m} \quad \text{and} \quad R_{3b}^{(j)} = \frac{(1 + s_0^2)^{1/2}}{(3/2)^{1/2} \kappa_*} (e^{\pi/s_0})^j, \quad (5)$$

where $j=0, 1, \dots$, labels each Efimov state according to their excitation, $\kappa_* \approx 0.226/r_{\text{vdW}}$ is the three-body parameter [54], and $e^{\pi/s_0} \approx 22.7$ is Efimov's geometric factor for identical bosons. In the unitary Bose gas, however, one expects that only Efimov states with binding energies larger than ϵ_n , and sizes smaller than k_n^{-1} are insensitive to the background gas and can exist in their free-space form. Otherwise, Efimov states should be sensitive to the background gas, represented here by a local trapping potential. To illustrate this sensitivity within our model, the energy levels, E_β , of three-identical bosons at $|a| = \infty$ as a function of n_{lo} are shown in Fig. 1(a), displaying geometric scaling as n_{lo} is increased by a factor $(e^{\pi/s_0})^3 \approx 1.17 \times 10^4$. Within our model, as the energy of a Efimov state approaches ϵ_n^{lo} its value is shifted away from its value in free-space [green dashed lines in Fig. 1(a)]. In order to describe loss processes within our

model, we have also provided a finite width (lifetime) for the states, Γ_β ($\tau_\beta = \hbar/\Gamma_\beta$), adjusted to reproduce the known behavior of the Efimov physics in ^{85}Rb [63] —see Supplementary Material [55].

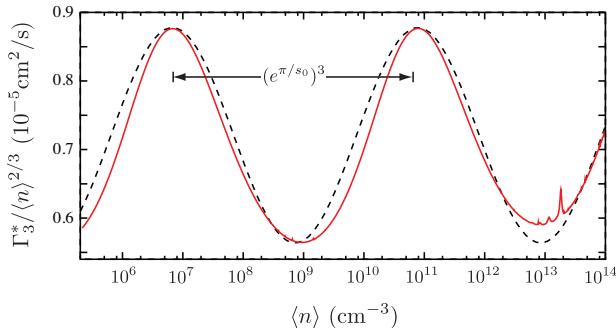


FIG. 2. Three-body decay rate, Γ_3^* , for ^{85}Rb at $|a| = \infty$ as a function of the average density, $\langle n \rangle$. This figure displays the $\langle n^{2/3} \rangle$ scaling of the decay rate as well as the appearance of log-periodic oscillations associated with Efimov physics. Resonances at higher $\langle n \rangle$ occur when the initial state is degenerate with one of the possibly weakly-coupled final states in our model. Dashed black curve is the fitting function in Eq. (8).

Besides the three-body eigenenergies, our model also provides wave functions that determine various properties of the quenched system. After quenching to the unitary regime, the time evolution of the three-body system is described by the projected three-body wave function,

$$\Psi(R, \Omega, t) = \sum_{\beta} c_{\beta}^{(u)} \psi_{\beta}^{(u)}(R, \Omega) e^{-i(E_{\beta} - i\Gamma_{\beta}/2)t/\hbar}, \quad (6)$$

which is a superposition of states at unitarity, $\psi_{\beta}^{(u)}$, with coefficients determined from their overlap with the initial state, $c_{\beta}^{(u)} = \langle \psi_{\beta}^{(u)} | \psi_i \rangle$. Within our local model, however, the wave function in Eq. (6) can only be expected to qualitatively represent the actual many-body system for $t < t_n$, since beyond this time scale genuine many-body effects should become important. Figure 1(c) shows the population at unitarity, $|c_{\beta}|^2$, for various states as a function of n_{lo} . We observe that the population of a given state becomes substantial when its energy or size is in the vicinity of the density-derived scales of the unitary Bose gas (ϵ_n and k_n^{-1} , respectively).

The above results suggest that Efimov physics may manifest in the density dependence of relevant observables since the atomic density sets the energy and length scales of the gas. We first focus on the three-body decay rates, which can be simply evaluated within our model from [17]

$$\Gamma_3^* = -\lim_{t \rightarrow 0} \frac{\dot{n}(t)}{n(t)} = \sum_{\beta} |c_{\beta}^{(u)}(n_{\text{lo}})|^2 \frac{\Gamma_{\beta}(n_{\text{lo}})}{\hbar}, \quad (7)$$

where $n(t) = n_{\text{lo}} |\langle \Psi(R, \Omega, t) | \Psi(R, \Omega, t) \rangle|$. In a local density model, the decay rate in Eq. (7) is averaged over

the local density n_{lo} . Using a Thomas-Fermi density profile, our numerical calculations indicate that the averaged rate is well approximated (within no more than 4%) by replacing n_{lo} with the corresponding average density $\langle n \rangle$ in Eq. (7). Our results for the three-body decay rate for the quenched unitary Bose gas are shown in Fig. 2, covering a broad range of densities. We find the expected $\langle n^{2/3} \rangle$ scaling [8, 19, 21] but also log-periodic oscillations that originate from the increase of an Efimov state population whenever its binding energy is comparable to ϵ_n (see Fig. 1). We fit these oscillations as

$$\Gamma_3^* \approx \eta \frac{\hbar}{m} \left[A + B \sin^2 \left(s_0 \ln \frac{\langle n \rangle^{1/3}}{r_{\text{vdW}}} + \phi \right) \right] \langle n^{2/3} \rangle \quad (8)$$

where $A \approx 15.9$, $B \approx 8.80$, and $\phi \approx 1.61$ —see dashed black curve in Fig. 2. Our numerical calculations, although largely log-periodic, are slightly asymmetric. The results shown in Fig. 2 have roughly 40% lower amplitude than the experimental decay rate for ^{85}Rb [8], however, the oscillation phase is consistent with preliminary experimental observations [64]. While our results account for losses at unitarity only, the experimental data was obtained after a B -field sweep to weak interactions [8], thus allowing for additional atom loss. Nevertheless, the existence of the log-periodic oscillations in Fig. 2, with a substantial amplitude, violates the universality hypothesis [11], in which all observables related to the unitary Bose gas should scale continuously as powers of n . Equation (8) depends only on the system parameters r_{vdW} and η for a particular atomic species.

We now shift our focus to the dynamical formation of weakly bound diatomic and Efimov states in quenched unitary Bose gases. In fact, in the recent ^{85}Rb experiment of Ref. [8] a population of such few-body bound states was obtained by quenching the system to unitarity, evolving for a time t_{dwell} , and subsequently sweeping the system back to weaker interactions ($a \approx 700a_0$) within a time t_{sw} . There is still, however, much to be understood on the dependence of populations on the various parameters (n , t_{dwell} , and t_{sw}) and the possible connections to the non-equilibrium dynamics in the unitary regime. In order to address some of these questions we focus initially on the case $t_{\text{sw}} \ll t_n$, where ramping effects are minimized, and solve the time-dependent three-body Schrödinger equation following the same experimental protocol of Ref. [8] described above —see also Refs. [55, 65]. Figure 3(a) shows the three-body energy spectrum for a given density and for a range of a relevant for the ^{85}Rb experiment. For this particular density, $\langle n \rangle \approx 9.9 \times 10^{10} \text{ cm}^{-3}$, only the ground- [$\beta = 0$, not shown in Fig. 3(a)] and first-excited Efimov states ($\beta = 1$) have sizes smaller than the average interatomic distance. The black solid line in Fig. 3(a) is the energy of the (free-space) diatomic state, $-\hbar^2/ma^2$, while the red curves following along this threshold correspond to atom-diatom states, and those following along the $E = 0$

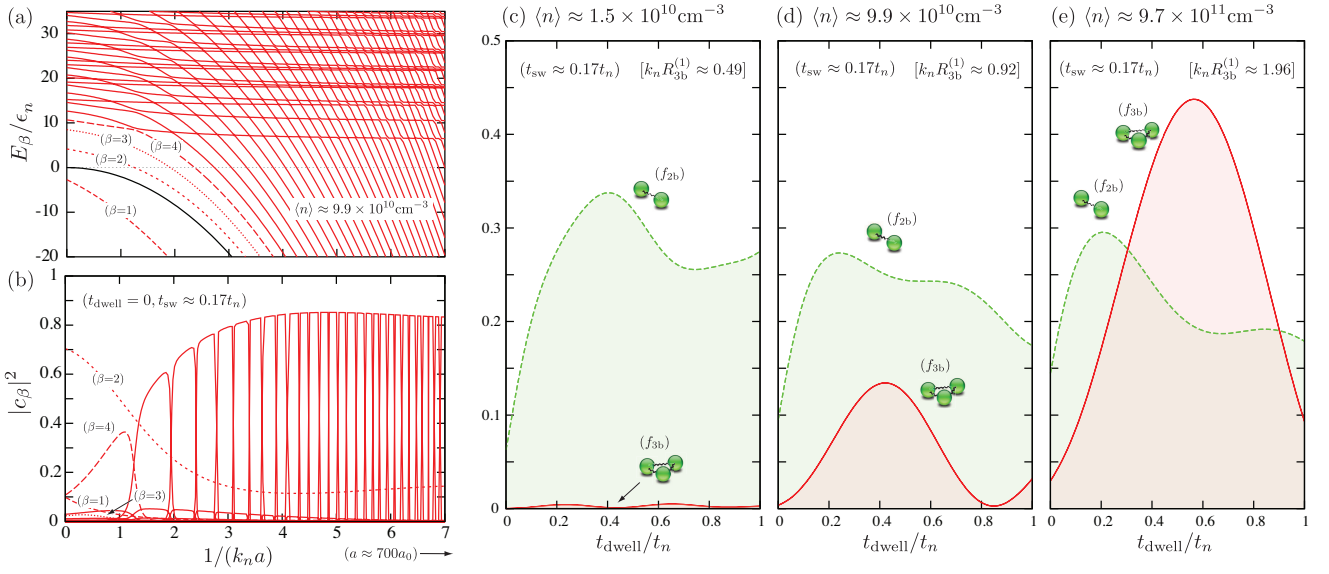


FIG. 3. (a) Three-body energy spectrum for $\langle n \rangle \approx 9.9 \times 10^{10} \text{ cm}^{-3}$ within a range of a relevant for the ^{85}Rb experiment. Black solid line corresponds to the energy of the (free-space) diatomic state (\hbar^2/ma^2). (b) Corresponding change of population during the field sweep ($t_{\text{sw}} \approx 0.17t_n$) obtained immediately after the quench ($t_{\text{dwell}} = 0$). (c)-(e) Population fraction of diatomic and Efimov states formed as a function of t_{dwell} illustrating the enhancement of Efimov state formation as the density approaches the characteristic value $\langle n_1^* \rangle \approx 5.2 \times 10^{10} \text{ cm}^{-3}$ [Eq. (9)] or, equivalently, when $k_n R_{3b} \approx 0.78(2)$ [30].

threshold correspond to three-atom states. Figure 3(b) shows the population changes during the sweep of the interactions ($t_{\text{sw}} \approx 0.17t_n$) from $|a| = \infty$ to $a \approx 700a_0$, for a case in which the system is not held in the unitary regime ($t_{\text{dwell}} = 0$). Whenever $t_{\text{dwell}} = 0$, the population of few-body bound states develops entirely during the interaction sweep. To quantify the population dynamics, we define the fraction of formed two-body states, $f_{2b} = (2/3) \sum_\beta |c_\beta|^2$, and Efimov states, $f_{3b} = \sum_\beta |c_\beta|^2$, after the sweep [55]. For the parameters of Fig. 3(b), we find that f_{2b} and f_{3b} are approximately 0.095 and 0.004, respectively, with the remaining fraction of atoms unbound.

To explore how the time-evolution of the system at unitarity impacts the formation of two- and three-body bound states, we study their dependence on t_{dwell} over a range of atomic densities [see shaded region in Fig. 1(b)]. Figure 3(c) shows that for a relatively low density where, although f_{2b} grows fast and reaches appreciable values, f_{3b} still remains negligible for all t_{dwell} . A larger population of Efimov states, however, is observed for higher densities [see Figs. 3(d) and (e), and Ref. [55].] In general, we find that for short-times $f_{2b} \propto t_{\text{dwell}}$ and $f_{3b} \propto t_{\text{dwell}}^2$, consistent with the early-time growth of two- and three-body correlations found in Ref. [30]. Also, in Ref. [30], it was observed that at early-times the largest enhancement of three-body correlations occurred at densities where the average interatomic distance is comparable to the size of an Efimov state. More precisely, this occurred when $k_n R_{3b} = 0.74(5)$, associated with a characteristic density

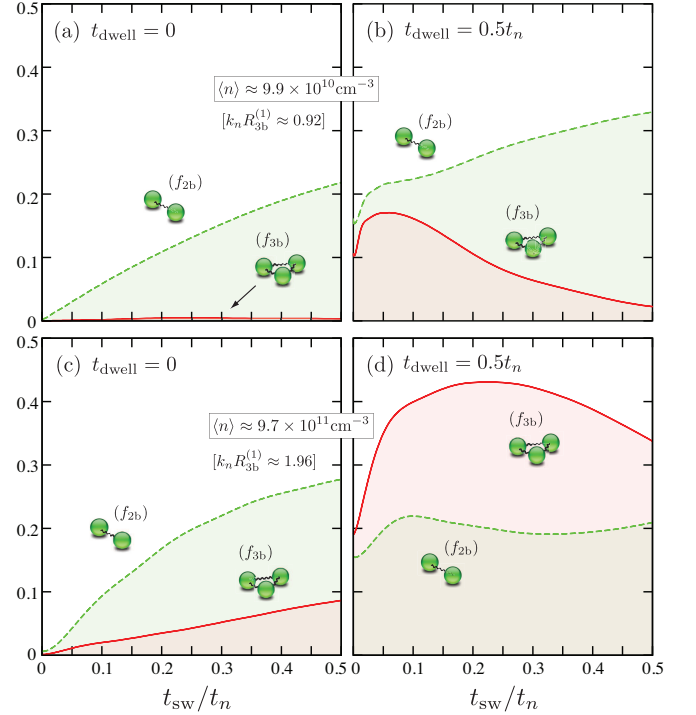


FIG. 4. Dependence of f_{2b} and f_{3b} on t_{sw} for (a)-(b) $\langle n \rangle \approx 9.9 \times 10^{10} \text{ cm}^{-3}$ and (c)-(d) $9.7 \times 10^{11} \text{ cm}^{-3}$. For $t_{\text{dwell}} = 0$, the dependence on t_{sw} is well described by the Landau-Zener results (see text) while for $t_{\text{dwell}} = 0.5t_n$ [(b) and (d)] the growth of correlations lead to the enhancement of the trimer population and a departure from the Landau-Zener results.

value

$$\langle n_j^* \rangle \approx 0.41 \frac{(3/2)^{1/2}}{4\pi^2(1+s_0^2)^{3/2}} \frac{\kappa_*^3}{(e^{\pi/s_0})^{3j}}. \quad (9)$$

For the range of densities explored in the ^{85}Rb experiment [8] the relevant characteristic density is $\langle n_1^* \rangle \approx 5.2 \times 10^{10} \text{cm}^{-3}$. In fact, Figs. 3 (c)-(e) display a marked change in the dynamics of f_{3b} as $\langle n_1^* \rangle$ is approached from below and then exceeded. In Figs. 3 (c)-(e) we also display the corresponding values for $k_n R_{3b}$. For densities beyond $\langle n_1^* \rangle$ (see also Ref. [55]) the population of Efimov states is clearly enhanced and can be attributed to the growth of few-body correlations [30]. Within our model, such enhancement is also consistent with the increase of population of the first-excited Efimov state at unitarity [see Fig. 1(b)].

Correlation growth can also be further studied by investigating the dependence of the populations on t_{sw} , shown in Fig. 4 for two densities and for $t_{\text{dwell}} = 0$ and $0.5t_n$. For $t_{\text{dwell}} = 0$ [Figs. 4(a) and (c)], i.e., in absence of time evolution at unitarity and the corresponding growth of correlations, the dependence of the populations on t_{sw} is well described by the Landau-Zener result: $f = f_m(1 - e^{-t_{\text{sw}}/t_m})$, where f_m is the final population and t_m the time scale related to the strength of the couplings between the states involved in the process [60, 66]. These findings are drastically changed as the system is allowed to evolve at unitarity, coinciding with the growth of few-body correlations [30]. In that case, as shown in Figs. 4(b) and (d), the population dynamics departs from the Landau-Zener results. For $t_{\text{dwell}} \neq 0$, there is a clear enhancement of f_{3b} —even at $t_{\text{sw}} = 0$ — which, in some cases [Fig. 4(d) and Ref. [55]], can lead to a population of Efimov states exceeding that of diatomic states.

In summary, solving the three-body problem in a local harmonic trap, designed to reflect density effects, we highlight the importance of Efimov physics in quenched unitary Bose gases. Within our model, the continuous scaling invariance of unitary Bose gases is violated in relevant three-body observables. In the three-body decay rates, this violation manifests through the appearance of log-periodic oscillations characteristic of the Efimov effect. In the early-time population growth of Efimov states after the system is swept away from unitarity it manifests through a marked change in dynamics as the density exceeds a characteristic value corresponding to a length scale matching that of the Efimov state size and interparticle spacing. Furthermore, our study characterizes the growth of correlations at unitarity through the early-time dynamics of the population of diatomic and Efimov states. This is shown to be qualitatively consistent with the early-time growth of two- and three-body correlations at unitarity observed in Ref. [30]. Moreover, we find that the departure from the Landau-Zener results for the populations in the non-equilibrium regime can also be associated with the increase of correlations in

the system. An experimental study of the predictions of our model is within the range of current quenched unitary Bose gas experiments.

The authors thank E. A. Cornell, C. E. Klauss, J. L. Bohn, J. P. Corson, D. Blume and S. Kokkelmans for extensive and fruitful discussions. J. P. D. acknowledges support from the U.S. National Science Foundation (NSF), Grant PHY-1607204, and from the National Aeronautics and Space Administration (NASA). V.E.C. acknowledges support from the NSF under Grant PHY-1734006 and by Netherlands Organization for Scientific Research (NWO) under Grant 680-47-623.

-
- [1] R. J. Fletcher, A. L. Gaunt, N. Navon, R. P. Smith, and Z. Hadzibabic, *Phys. Rev. Lett.* **111**, 125303 (2013).
 - [2] B. S. Rem, A. T. Grier, I. Ferrier-Barbut, U. Eismann, T. Langen, N. Navon, L. Khaykovich, F. Werner, D. S. Petrov, F. Chevy, and C. Salomon, *Phys. Rev. Lett.* **110**, 163202 (2013).
 - [3] P. Makotyn, C. E. Klauss, D. L. Goldberger, E. A. Cornell, and J. D. S., *Nat. Phys.* **10**, 116 (2014).
 - [4] U. Eismann, L. Khaykovich, S. Laurent, I. Ferrier-Barbut, B. S. Rem, A. T. Grier, M. Delehaye, F. Chevy, C. Salomon, L.-C. Ha, and C. Chin, *Phys. Rev. X* **6**, 021025 (2016).
 - [5] F. Chevy and C. Salomon, *J. Phys. B* **49**, 192001 (2016).
 - [6] R. J. Fletcher, R. Lopes, J. Man, N. Navon, R. P. Smith, M. W. Zwierlein, and Z. Hadzibabic, *Science* **355**, 377 (2017).
 - [7] S. Laurent, M. Pierce, M. Delehaye, T. Yefsah, F. Chevy, and C. Salomon, *Phys. Rev. Lett.* **118**, 103403 (2017).
 - [8] C. E. Klauss, X. Xie, C. Lopez-Abadia, J. P. D’Incao, Z. Hadzibabic, D. S. Jin, and E. A. Cornell, *Phys. Rev. Lett.* **119**, 143401 (2017).
 - [9] C. Eigen, J. A. P. Glidden, R. Lopes, N. Navon, Z. Hadzibabic, and R. P. Smith, *Phys. Rev. Lett.* **119**, 250404 (2017).
 - [10] R. J. Fletcher, J. Man, R. Lopes, P. Christodoulou, J. Schmitt, M. Sohmen, N. Navon, R. P. Smith, and Z. Hadzibabic, *arxiv:1803.06338* (2018).
 - [11] T.-L. Ho, *Phys. Rev. Lett.* **92**, 090402 (2004).
 - [12] J. M. Diederix, T. C. F. van Heijst, and H. T. C. Stoof, *Phys. Rev. A* **84**, 033618 (2011).
 - [13] W. Li and T.-L. Ho, *Phys. Rev. Lett.* **108**, 195301 (2012).
 - [14] S.-J. Jiang, W.-M. Liu, G. W. Semenov, and F. Zhou, *Phys. Rev. A* **89**, 033614 (2014).
 - [15] S. Laurent, X. Leyronas, and F. Chevy, *Phys. Rev. Lett.* **113**, 220601 (2014).
 - [16] X. Yin and L. Radzihovsky, *Phys. Rev. A* **88**, 063611 (2013).
 - [17] A. G. Sykes, J. P. Corson, J. P. D’Incao, A. P. Koller, C. H. Greene, A. M. Rey, K. R. A. Hazzard, and J. L. Bohn, *Phys. Rev. A* **89**, 021601 (2014).
 - [18] M. Rossi, L. Salasnich, F. Ancilotto, and F. Toigo, *Phys. Rev. A* **89**, 041602 (2014).
 - [19] D. H. Smith, E. Braaten, D. Kang, and L. Platter, *Phys. Rev. Lett.* **112**, 110402 (2014).
 - [20] E. Braaten, D. Kang, and L. Platter, *Phys. Rev. Lett.* **106**, 153005 (2011).

- [21] F. Werner and Y. Castin, Phys. Rev. A **86**, 053633 (2012).
- [22] S. Piatecki and W. Krauth, Nat. Comm **5**, 3503 (2014).
- [23] M. Kira, Nat. Comm. **6**, 6624 (2015).
- [24] M. Barth and J. Hofmann, Phys. Rev. A **92**, 062716 (2015).
- [25] J. P. Corson and J. L. Bohn, Phys. Rev. A **91**, 013616 (2015).
- [26] T. Comparin and W. Krauth, Phys. Rev. Lett. **117**, 225301 (2016).
- [27] X. Yin and L. Radzihovsky, Phys. Rev. A **93**, 033653 (2016).
- [28] S.-J. Jiang, J. Maki, and F. Zhou, Phys. Rev. A **93**, 043605 (2016).
- [29] Y. Ding and C. H. Greene, Phys. Rev. A **95**, 053602 (2017).
- [30] V. E. Colussi, J. P. Corson, and J. P. D’Incao, Phys. Rev. Lett. **120**, 100401 (2018).
- [31] M. W. C. Sze, A. G. Sykes, D. Blume, and J. L. Bohn, Phys. Rev. A **97**, 033608 (2018).
- [32] D. Blume, M. W. C. Sze, and J. L. Bohn, Phys. Rev. A **97**, 033621 (2018).
- [33] C. Chin, R. Grimm, P. Julienne, and E. Tiesinga, Rev. Mod. Phys. **82**, 1225 (2010).
- [34] S. Giorgini, L. P. Pitaevskii, and S. Stringari, Rev. Mod. Phys. **80**, 1215 (2008).
- [35] M. Holland, S. J. J. M. F. Kokkelmans, M. L. Chiofalo, and R. Walser, Phys. Rev. Lett. **87**, 120406 (2001).
- [36] S. J. J. M. F. Kokkelmans, J. N. Milstein, M. L. Chiofalo, R. Walser, and M. J. Holland, Phys. Rev. A **65**, 053617 (2002).
- [37] J. P. D’Incao, H. Suno, and B. D. Esry, Phys. Rev. Lett **93**, 123201 (2004).
- [38] A. Polkovnikov, K. Sengupta, A. Silva, and M. Vengalattore, Rev. Mod. Phys. **83**, 863 (2011).
- [39] M. Rigol, V. Dunjko, and M. Olshanii, Nature **452**, 854 (2008).
- [40] J. Dziarmaga, Advances in Physics **59**, 1063 (2010).
- [41] M. Gring, M. Kuhnert, T. Langen, T. Kitagawa, B. Rauer, M. Schreitl, I. Mazets, D. A. Smith, E. Demler, and J. Schmiedmayer, Science **337**, 1318 (2012).
- [42] M. A. Cazalilla, A. Iucci, and M.-C. Chung, Phys. Rev. E **85**, 011133 (2012).
- [43] W. H. Zurek, U. Dorner, and P. Zoller, Phys. Rev. Lett. **95**, 105701 (2005).
- [44] V. Efimov, Sov. J. Nuc. Phys. **29**, 546 (1979).
- [45] V. Efimov, Nucl. Phys. A **210**, 157 (1973).
- [46] E. Braaten and H. W. Hammer, Phys. Rep. **428**, 259 (2006).
- [47] Y. Wang, J. P. D’Incao, and B. D. Esry, Adv. At. Mol. Opt. Phys. **62**, 1 (2013).
- [48] P. Naidon and S. Endo, Rep. Prog. Phys. **80**, 056001 (2017).
- [49] J. P. D’Incao, J. Phys. B **51**, 043001 (2018).
- [50] C. H. Greene, P. Giannakeas, and J. Pérez-Ríos, Rev. Mod. Phys. **89**, 035006 (2017).
- [51] H. Suno, B. D. Esry, C. H. Greene, and J. P. Burke, Phys. Rev. A **65**, 042725 (2002).
- [52] J. P. D’Incao and B. D. Esry, Phys. Rev. A **72**, 032710 (2005).
- [53] J. Wang, J. P. D’Incao, and C. H. Greene, Phys. Rev. A **84**, 052721 (2011).
- [54] J. Wang, J. P. D’Incao, B. D. Esry, and C. H. H. Greene, Phys. Rev. Lett. **108**, 263001 (2012).
- [55] Supplemental Material [url:] for details of our model and implementation, which includes Refs. [67–71].
- [56] P. Naidon, S. Endo, and M. Ueda, Phys. Rev. A **90**, 022106 (2014).
- [57] P. Naidon, S. Endo, and M. Ueda, Phys. Rev. Lett. **112**, 105301 (2014).
- [58] K. Góral, T. Köhler, S. A. Gardiner, E. Tiesinga, and k. P. S. Julienne, J. Phys. B **37**, 3457 (2004).
- [59] B. Borca, D. Blume, and C. H. Greene, New J. Phys. **5**, 111 (2003).
- [60] J. von Stecher and C. H. Greene, Phys. Rev. Lett. **99**, 090402 (2007).
- [61] F. Werner and Y. Castin, Phys. Rev. Lett. **97**, 150401 (2006).
- [62] D. Blume, Rep. Prog. Phys. **75**, 046401 (2012).
- [63] R. J. Wild, P. Makotyn, J. M. Pino, E. A. Cornell, and D. S. Jin, Phys. Rev. Lett. **108**, 145305 (2012).
- [64] C. E. Klauss, *Resonantly Interacting Degenerate Bose Gas Oddities*, Ph.D. thesis, University of Colorado (2017), fig. 5.26 (<http://jila.colorado.edu/publications/62877/resonantly-interacting-degenerate-bose>).
- [65] J. E. Bækhoj, O. I. Tolstikhin, and L. B. Madsen, J. Phys. B **47**, 075007 (2014).
- [66] C. W. Clark, Phys. Lett. A **70**, 295 (1979).
- [67] E. G. M. van Kempen, S. J. J. M. F. Kokkelmans, D. J. Heinzen, and B. J. Verhaar, Phys. Rev. Lett. **88**, 093201 (2002).
- [68] N. R. Claussen, S. J. J. M. F. Kokkelmans, S. T. Thompson, E. A. Donley, E. Hodby, and C. E. Wieman, Phys. Rev. A **67**, 060701 (2003).
- [69] J. V. Lill, G. A. Parker, and J. C. Light, Chem. Phys. Lett. **89**, 483 (1982).
- [70] T. N. Rescigno and C. W. McCurdy, Phys. Rev. A **62**, 032706 (2000).
- [71] D. E. Manolopoulos and R. E. Wyatt, Chem. Phys. Lett. **152**, 23 (1988).